

MODELLING OF 'SATELLITE-TO-AIRCRAFT' LINK FOR SELF-SEPARATION

Volodymir Kharchenko, Yurii Barabanov, Andrii Grekhov

Dept of Air Navigation Systems, National Aviation University, Kosmonavta Komarova ave 1, 03680 Kyiv, Ukraine

Submitted 15 February 2013; accepted 8 April 2013

Abstract. The aim of this paper is to design the original model of communication channel 'Satellite-to-Aircraft' for self-separation with error-control coding using *MATLAB Simulink* software. Studying the signal transmission through a communication channel without coding and with convolutional coding the following parameters were changed: losses in a free space from 0 dB to 225 dB; noise temperature of an aircraft receiver 20 K and 290 K; simultaneous changing of antennas diameter; phase offsets from 0° to 20°; nonlinearity of satellite high power amplifier; satellite phase noise; and a data bit rate. BER is vanishing for free space path losses changing from 0 dB to 221 dB at the use of convolutional coding and a noise temperature 20 K, for diameters of all antennas of more than 1.2 m, and at phase shifts up to 4°. The signal constellation shows a presence of strong distortions during signal transmission. The proposed model can be used as a basic model for investigation of communication between two unmanned aircraft systems.

Keywords: free-flight, self-separation, ADS-B, BER, communication channel, aircraft, satellite, convolutional encoder, BPSK, free space loss, phase/frequency offset, memory-less nonlinearity, phase noise, Viterbi decoder, amplifier back-off level, noise temperature, antenna diameter.

Reference to this paper should be made as follows: Kharchenko, V.; Barabanov, Y.; Grekhov, A. 2013. Modelling of 'satellite-to-aircraft' link for self-separation, *Transport* 28(4): 361–367. <http://dx.doi.org/10.3846/16484142.2013.864699>

Introduction

Self-separation is an operational concept within the Free Flight initiative (RTCA 1995) which involves rules of the air, communication technologies, protocols, air traffic management and others (ICAO 2011).

Key technological aspect of a self-separation is Automatic Dependent Surveillance-Broadcast (ADS-B), in which aircraft transmits periodic position and state reports (RTCA 2002; EUROCONTROL 2012). ADS-B In refers to an appropriately equipped aircraft's ability to receive and display another aircraft's ADS-B Out information as well as the ADS-B In services provided by ground systems, including Automatic Dependent Surveillance-Rebroadcast (ADS-R), Traffic Information Service-Broadcast (TIS-B), and, if so equipped, Flight Information Service-Broadcast (FIS-B). When displayed in the cockpit, this information greatly improves the pilot's situational awareness in aircraft not equipped with a Traffic Alert and Collision Avoidance System (TCAS) or Airborne Collision Avoidance System (ACAS) (Federal Aviation Administration 2010).

ACAS is designed to work both autonomously and independently of the aircraft navigation equipment and autopilot systems as well as any ground systems used for the provision of air traffic services. Through antennas, ACAS interrogates the ICAO standard compliant transponders of aircraft in the vicinity. Based upon the replies received, the system tracks the slant range, altitude (when it is included in the reply message) and bearing of surrounding traffic (ACAS II Guide... 2012). TCAS is intended only for collision avoidance, but self-separation requires complex processing logic, time anticipation and procedure changes. Self-separation feasibility is dependent on confidence in automation and its co-existence with the human role in the cockpit.

Another technical concept for the association between self-separation and ADS-B was called Airborne Separation Assistance System (ASAS) which performs the core logic of self-separation and other related applications (CARE-ASAS/EUROCONTROL/99-001 2004).

The safe integration of Unmanned Aircraft Systems (UAS) into non-segregated airspace would be impossible

without new technologies for detecting and avoiding systems and frequency spectrum protection from unintentional or unlawful interference (Third Unmanned Aircraft... 2011; Towards a European Strategy... 2012). Remotely Piloted Aircraft (RPA) can be integrated in the international civil aviation in the foreseeable future. The Remotely Piloted Aircraft Systems (RPAS) Roadmap will provide a strategy for achieving RPAS integration into the European air system from 2016 (Remotely Piloted Aircraft... 2012). Problems caused by UAS flights in the common airspace are connected with the necessity of reliable real time control during the flight. Communication links for RPA are shown in Fig. 1.

UAS flights in the common airspace from our point of view globally can be provided by ADS-B Out/In, TIS-B, FIS-B using low Earth orbit satellite constellations for self-separation data transition.

One of such constellation is global satellite communication service Iridium (Manual for ICAO... 2007), which allows aviation users to send and receive voice, messaging and data regardless of their positions on or above the earth: air-to-land, land-to-air and air-to-air.

On 20 June 2012 satellite operator Iridium has decided that from 2015 they will be putting ADS-B receivers on its next-generation satellite constellation, aimed at bringing global, real-time aircraft surveillance for air navigation service providers (Feliz 2012).

Telecommunications satellite systems are widely used in aviation due to advantages of satellite communication which is connected with possibility of operating with many airplanes at long distances and with independence of communication expenses on distances to airplanes (An Introduction to Aircraft... 2009; Manual on Detailed Technical... 2010; Roddy 2006; Woolner 2003).

Modelling of ADS-B messages transmission without error-control coding and analysis of unmanned aircraft systems application in the civil field were realized previously in our papers (Kharchenko *et al.* 2012a, b, c; Kharchenko, Prusov 2012).

The aim of this paper is:

- to design the model of communication channel 'Satellite-to-Aircraft' for self-separation with

error-control coding using *MATLAB Simulink* software;

- to receive dependences of a Bit-Error Rate (BER) on a free space path loss, a phase/frequency offsets, a satellite transponder high power amplifiers back-off level, antennas diameter, a phase noise, a noise temperature, and a bit rate;
- to analyse the end-to-end signal constellations.

1. Model for 'Satellite-to-Aircraft' Link

The Iridium system includes 66 low-orbit satellites at an altitude of 780 km which are equally divided into 6 orbital planes (Iridium Satellites 2008). Each satellite can communicate with the Airborne Earth Station. Each satellite uses three phased-array antennas for the user links. These arrays are designed to provide user-link service by communicating within the 1616÷1626.5 MHz band (Osborne, Xie 1999). The gateway serves as a gateway to the Aviation Telecommunication Network for forwarding messages from the aircraft to the required Air Traffic Command or Aircraft Operational Communication unit.

Channels are implemented in the Iridium Satellite Network using a hybrid Time Division Multiple Access/Frequency Division Multiple Access architecture based on Time Division Duplex using a 90 millisecond frame and a Binary Phase-Shift Keyed (BPSK) modulation scheme (or DE-QPSK differential encoding).

A model for satellite communication channel 'Satellite-to-Aircraft' was built using *MATLAB Simulink* software and demo model 'RF Satellite Link'. The original model, shown in Fig. 2 comprises of 'Satellite Downlink Transmitter' (Bernoulli Random Binary Generator, Convolutional Encoder, BPSK Baseband Modulator, High Power Amplifier (HPA) with a memoryless non-linearity, Phase Noise, Transmitter Dish Antenna Gain), 'Downlink Path' (Free Space Path Loss, Phase/Frequency Offset), 'Aircraft Downlink Receiver' (Receiver Dish Antenna Gain, Ground Receiver System Temperature, Viterbi Decoder), 'Error Rate Calculation block' and 'Display'.

In the 'Satellite Downlink Transmitter' the Bernoulli Binary Generator block generates random binary numbers using a Bernoulli distribution with parameter p , produces 'zero' with probability p and 'one' with probability $1-p$ (the value $p = 0.5$ is used). The output signal is a frame-based matrix. The Bernoulli Binary Generator block generates a discrete signal and updates the signal at integer multiples of a fixed time interval, called the sample time. The length of this time interval has the value of 1 second with the exception of data transmission with different rates. The output data type is 'double'.

Iridium system employs a BPSK modulation and forward error correction coding in the form of convolutional encoding with Viterbi decoding (Viterbi 1971). Iridium uses a rate $3/4$, constraint length 7, ($r = 3/4$; $K = 7$) convolutional code on both transmission and reception (Costello *et al.* 1998). The Convolutional Encoder block is using the poly2trellis (7, [171 133], 171) function with a constraint length of 7, code generator

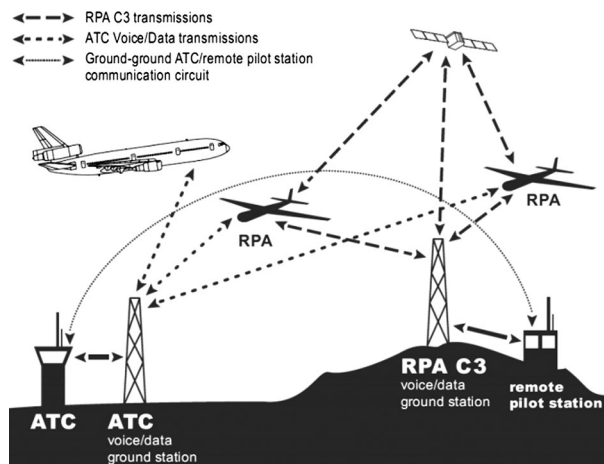


Fig. 1. Communication links (ICAO 2011)

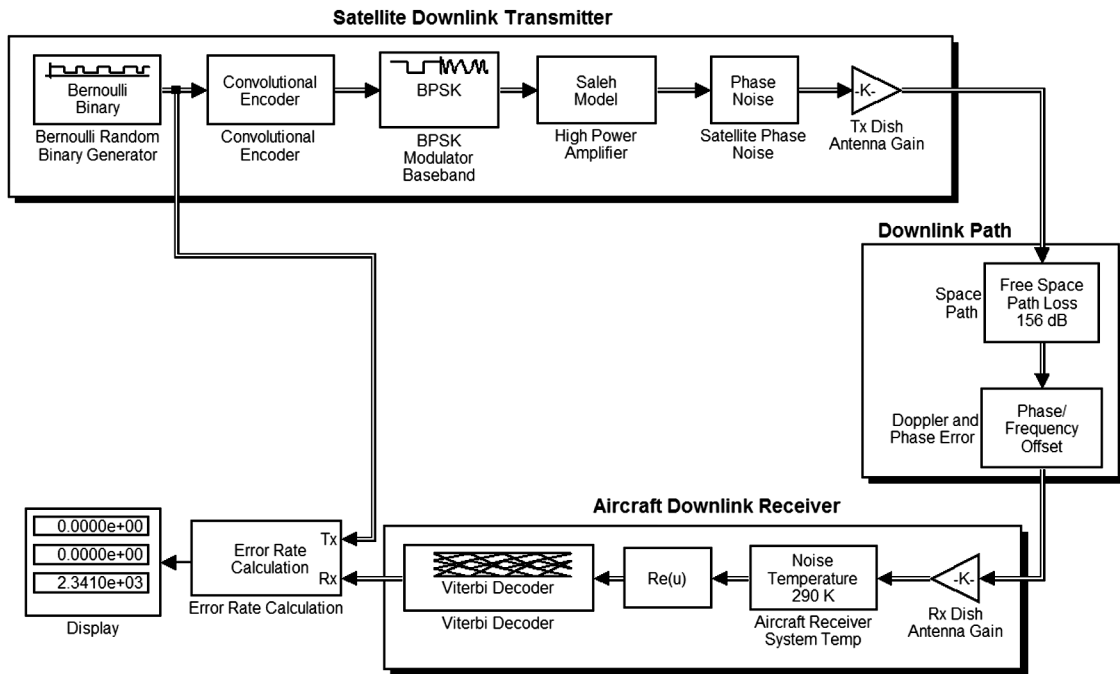


Fig. 2. ‘Satellite-to-Aircraft’ Link

polynomials of 171 and 133 (in octal numbers), and a feedback connection of 171 (in octal). The puncture vector is [1; 1; 0; 1; 1; 0].

The BPSK Baseband Modulator block modulates a signal using the binary phase shift keying method. The output is a baseband representation of the modulated signal.

The High Power Amplifier block applies memory-less nonlinearity to complex baseband signal and provides five different methods for modelling the nonlinearity. In this paper results only for Saleh model with standard AM/AM and AM/PM parameters are given (Saleh 1981). A HPA back-off level is used to determine how close the satellite high power amplifier is driven to saturation. The following selected back-off is used to set the input and output gain of the Memory-less Nonlinearity block: 30 dB – the average input power is 30 decibels below the input power that causes amplifier saturation (in this case AM/AM and AM/PM conversion is negligible); 7 dB – moderate nonlinearity; 1 dB – severe nonlinearity.

The Phase Noise block adds receiver phase noise to a complex baseband signal. The block applies the phase noise as follows: generates additive white Gaussian noise and filters it with a digital filter; adds the resulting noise to the angle component of the input signal. The level of the spectrum is specified by the noise power contained in a one hertz bandwidth offset from a carrier by a certain frequency. Modelling was provided for three levels: negligible (phase noise level: -100 dBc/Hz, frequency offset: 100 Hz), low (phase noise level: -55 dBc/Hz, frequency offset: 100 Hz), high (phase noise level: -48 dBc/Hz, frequency offset: 100 Hz).

The Transmitter (Receiver) Dish Antenna Gain block multiplies the input by a constant value (gain).

Dependencies of a BER on transmitting and receiving antennas diameter were obtained using vectors $[d_1, d_2]$ for each pair ‘transmitter-receiver’. The first element in the vector $[d_1, d_2]$ represents the transmitting antenna diameter (in meters) and is used to calculate the gain in the Transmitter Dish Antenna Gain block. The second element represents the receiving antenna diameter and is used to calculate the gain in the Receiver Dish Antenna Gain block. The default setting is [1.0, 1.0] (an antenna gain is 12.4) and diameters of all antennas (transmitting antenna on a satellite and receiving antenna on an aircraft) were changed simultaneously.

In the ‘Downlink Path’ the Free Space Path Loss block simulates the loss of signal power due to the distance between the satellite transmitter and aircraft receiver. The block reduces the amplitude of the input signal by an amount that is determined by the Loss (dB) parameter.

The Phase/Frequency Offset block applies phase and frequency offsets to an incoming signal.

In the ‘Aircraft Downlink Receiver’ the Viterbi Decoder block decodes input symbols to produce binary output symbols. Unquantized decision type parameter was used.

Comparing scatter plots of the signal after BPSK modulation and before demodulation allows viewing the impact of all impairments on the received signal.

2. Aeronautical Satellite Channel Simulation

For computer modelling a distance between the Iridium satellite and the aircraft 780 km and an operational frequency 1616 MHz were taken. Changing a carrier frequency of the link updates the Free Space Path Loss block.

Free-space path loss is the loss in signal strength that results from a line-of-sight path through free space. Free-space path loss does not include the gain of the antennas used at the transmitter and receiver. Free-space path loss is proportional to the square of the distance between the transmitter and receiver, and also proportional to the square of Iridium operational frequency. A dependence of a BER on free space path loss for different noise temperatures without coding and with convolutional coding is shown in Fig. 3. Convolutional coding considerably decreases errors probability and a BER is vanishing for free space path loss in the range from 0 dB to 221 dB (in case of very low noise temperature 20 K) and from 0 dB to 208 dB (in case of typical noise temperature 290 K).

Changing of all antennas diameter has significant influence on errors probability shown in Fig. 4 – the bigger antennas diameter is, the lower is an error probability. In this simulation free space path loss was fixed, HPA nonlinearity – moderate, and two noise temperatures were considered.

Convolutional coding essentially reduces the error probability that leads to a BER vanishing for antennas with diameter of more than 1.2 m. Iridium satellite has three Main Mission Antennas (each of 0.86 m wide and 1.86 m high) (Iridium Satellites 2008). The same area has

a circle with a diameter ≈ 1.4 m. Apparently, results of our modelling are in the good consent with these data.

In the presence of an arbitrary phase offset introduced by the downlink, the demodulator is unable to tell which constellation point is which. A dependence of a BER on phase offset in the downlink is shown in Fig. 5 for two noise temperatures without convolutional coding and with it. At using convolutional coding a BER is vanishing for phase shifts up to 4° at downlink losses in free space 250 dB and a noise temperature of aircraft receiver 290 K. Signal constellations for BPSK modulation scheme at the phase offset 20° in the downlink is shown in Fig. 6.

Setting the Phase Noise parameter to the high level (phase noise level: -48 dBc/Hz, frequency offset 100 Hz) leads to the increased variance in the tangential direction in the received signal scatter plot shown in Fig. 7. Setting the Phase Noise to the low level (phase noise level: -55 dBc/Hz, frequency offset 100 Hz) leads to a situation when the variance in the tangential direction has somewhat decreased. This level of phase noise is not sufficient to cause errors.

In proposed model satellite HPA is amplifying a signal on the downlink side of Iridium communications satellite by the model of a Traveling Wave Tube Amplifier (TWTA) using the Saleh model. For an input sine

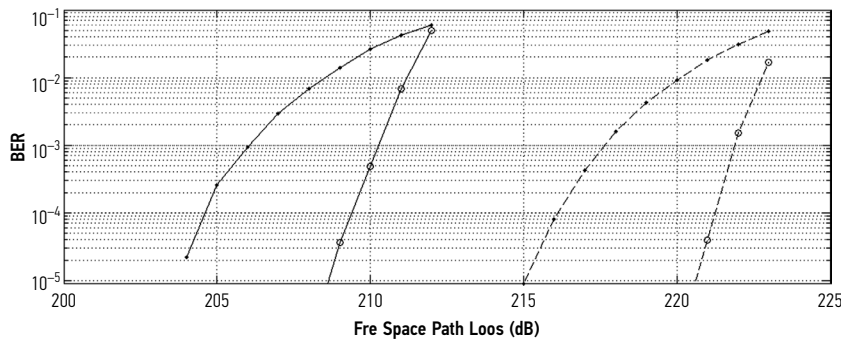


Fig. 3. Dependence of an error probability for a BPSK modulation scheme on free space path loss: dots – without coding, circles – with convolutional coding (rate 3/4, constraint length $K = 7$); receiver noise temperature is 20 K (dashed lines) and 290 K (solid lines); HPA back-off level is 7 dB; phase and frequency offsets are equal to zero; antennas gain $G = 1$; satellite phase noise is negligible

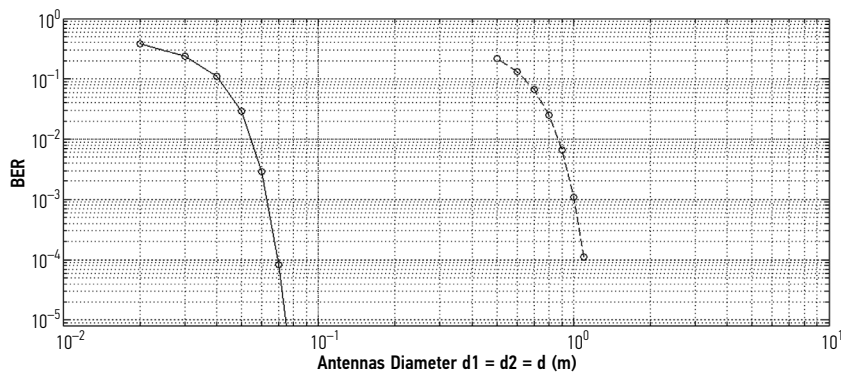


Fig. 4. Dependence of error probability for a BPSK modulation scheme on satellite and aircraft antennas diameter: circles – with convolutional coding (rate 3/4, constraint length $K = 7$); receiver noise temperature is 20 K (dashed lines) and 290 K (solid lines); phase and frequency offsets are equal to zero; HPA back-off level is 7 dB; free space path loss is 250 dB; satellite phase noise is negligible

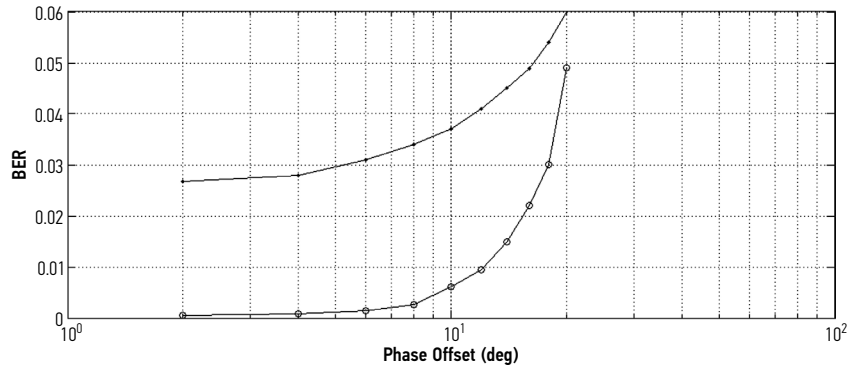


Fig. 5. Dependence of error probability for BPSK modulation scheme on a phase offset in the downlink: dots – without coding, circles – with convolutional coding (rate 3/4, constraint length $K = 7$); receiver noise temperatures 290 K, free space path loss 250 dB; HPA back-off level 7 dB; frequency offset is equal to zero; antennas gain $G = 10$; satellite phase noise is negligible

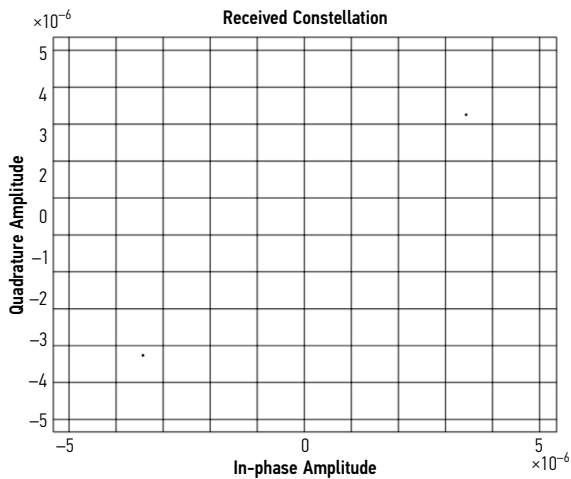


Fig. 6. End signal constellation for BPSK modulation scheme for a phase offset 20° in the downlink: with convolutional coding (rate 3/4, constraint length $K = 7$); aircraft receiver noise temperature 0 K; free space path loss 160 dB; HPA back-off level 7 dB; frequency offset is equal to zero; $d_1 = d_2 = 1.0$ m; satellite phase noise is negligible

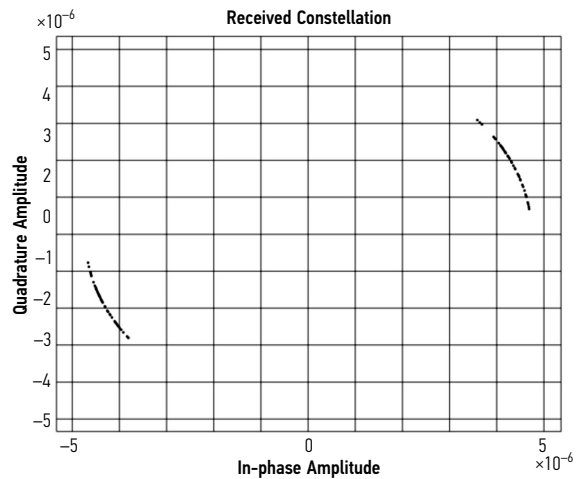


Fig. 7. Signal constellation for BPSK modulation scheme for the high level of phase noise (-48 dBc/Hz, frequency offset 100 Hz): with convolutional coding (rate 3/4, constraint length $K = 7$); aircraft receiver noise temperatures 0 K; free space path loss 160 dB; HPA back-off level 7 dB; phase offset is equal to zero; $d_1 = d_2 = 1.0$ m

wave of frequency f and amplitude r , the TWTA is characterized by the relationship (Elbert, Schiff 2003):

$$y(t) = A(r) \cdot \sin(2 \cdot \pi \cdot f \cdot t + \varphi(r)),$$

where the empirical relations:

$$A(r) = \frac{a_r \cdot r}{1 + b_r \cdot r^2};$$

$$\varphi(r) = \frac{a_\varphi \cdot r^2}{1 + b_\varphi \cdot r^2}$$

describe $A(r)$ and $\varphi(r)$. The first term is called AM/AM conversion, and the second is AM/PM conversion. The four constants:

$$a_r = 2.1587;$$

$$b_r = 1.1517;$$

$$a_\varphi = 4.0330;$$

$$b_\varphi = 9.1040.$$

Nonlinear method options in the block apply a memory-less nonlinearity to the complex baseband input signal in the following manner: multiplies the signal by a gain factor; splits the complex signal into its magnitude and angle components; applies an AM/AM conversion to the magnitude of the signal, according to the Saleh nonlinearity method (Saleh 1981), to produce the magnitude of the output signal; applies an AM/PM conversion to the phase of the signal, according to the Saleh nonlinearity method, and adds the result to the angle of the signal to produce the angle of the output signal; combines the new magnitude and angle components into a complex signal and multiplies the result by a gain factor, which is controlled by the Linear gain parameter. A dependence of a BER on nonlinearities of satellite HPA is shown in Table.

For modelling a data transmission with different rates it is possible to change sample time in the Bernoulli Binary Generator block. The sample time is a parameter that indicates when, during simulation, the block

Table. Dependence of error probability for BPSK modulation scheme on satellite HPA nonlinearity

HPA back-off level	BER (Aircraft Receiver Noise Temperatures $T = 20$ K)			BER (Aircraft Receiver Noise Temperatures $T = 290$ K)		
	Free Space Path Loss			Free Space Path Loss		
	210 dB	214 dB	225 dB	203 dB	206 dB	212 dB
30 dB (negligible nonlinearity)	0.0	0.0	0.0	0.0	0.0	0.0
7 dB (moderate nonlinearity)	0.0	0.0	$2.78 \cdot 10^{-1}$	0.0	0.0	$5.43 \cdot 10^{-2}$
1 dB (severe nonlinearity)	0.0	$1.89 \cdot 10^{-2}$	$4.93 \cdot 10^{-1}$	$5.98 \cdot 10^{-2}$	$4.26 \cdot 10^{-1}$	$4.980 \cdot 10^{-1}$

Note: Antennas gain $G = 1$; with convolutional coding (rate 3/4, constraint length $K = 7$); without phase and frequency offsets.

produces outputs. So, a value inversely proportional to a sample time will give a number of samples per second and can be considered as equivalent of a bit rate. In Fig. 8 a dependence of a BER on a bit rate for different free space path losses is shown.

Conclusions

For modelling of a self-separation a transmission of ADS-B messages on the base of low-orbit satellite constellation Iridium the original model of a communication channel 'Satellite-to-Aircraft' with error-control coding was built using *MATLAB Simulink* software.

For studying of a signal transmission through a communication channel without coding and with convolutional coding the following parameters were changed: losses in a free space from 0 dB to 225 dB (Fig. 3); noise temperature of an aircraft receiver (20 K, 290 K); simultaneous changing of antennas diameter that increased or reduced a power of the received signal (Fig. 4); phase offsets from 0° to 20° (Figs 5, 6); nonlinearity of satellite HPA (Table); satellite phase noise (Fig. 7); and a data bit rate (Fig. 8).

Signal changes were analysed by means of active windows-indicators which allowed defining a BER and constellations of the transmitted and received signals (Figs 6, 7).

Dependencies shown in Figs 3–8 were obtained for 'standard parameters': without coding and with convolutional coding (rate 3/4, constraint length $K = 7$); noise temperatures 20 K and 290 K; negligible HPA; and negligible phase noise. Values of free space path losses, phase and frequency offsets, antennas diameter were specified in each special case.

For 'standard parameters' a BER is vanishing for free space path losses changing from 0 dB to 221 dB at use of convolutional coding and a noise temperature 20 K (Fig. 3). This result is in good agreement with a satellite communication channel budget (Sklar 2001).

Antennas diameter essentially influence on a BER (Fig. 4). The probability of errors for 'standard parameters' is vanishing for diameters of all antennas of more than 1.2 m. This result is in good agreement with the size of Iridium satellite antennas (Iridium Satellites 2008).

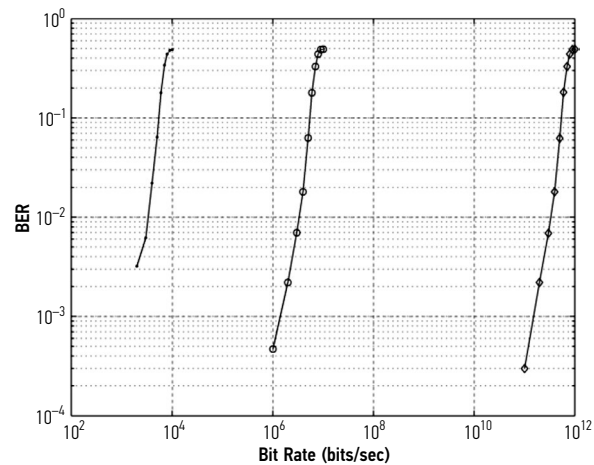


Fig. 8. Dependence of error probability for a BPSK modulation scheme on data transmission rate: free space path loss 180 dB (dots), 150 dB (circles), 100 dB (diamonds); with convolutional coding (rate 3/4, constraint length $K = 7$); receiver noise temperature is 290 K; phase and frequency offsets are equal to zero; HPA back-off level is 7 dB; satellite phase noise is negligible; antennas gain $G = 1$

Influence of convolutional coding on dependence of a BER on phase offsets in the link is critical and changes character of this dependence (Fig. 5), essentially reducing the level of errors. Under 'standard parameters' and noise temperature 290 K a BER is vanishing at phase shifts up to 4° . The signal constellation (Fig. 6) shows a presence of strong distortions during signal transmission.

Influence of HPA backoff parameter on a BER was studied for different free space losses and noise temperatures (Table). In this case the gain of antennas was $G = 1$.

The impact of phase noise on a transmitted signal is shown in Fig. 8.

The proposed model can be used as basic model for investigation of communication between two unmanned aircraft systems and ground stations using several satellites. Developed model can also be used for finding optimal methods of error-correcting coding.

This paper covers evaluation of 'Satellite-to-Aircraft' link performance which can be used for self-separation of unmanned aircraft systems (in particular for remotely piloted aircraft).

References

- ACAS II Guide: Airborne Collision Avoidance System II (Incorporating Version 7.1). 2012. Available from Internet: http://www.eurocontrol.int/msa/gallery/content/public/documents/ACAS_guide71.pdf
- An Introduction to Aircraft Satellite Tracking. 2009. Available from Internet: http://www.indigosat.com/marketing/About_satellite_tracking.pdf
- CARE-ASAS/EUROCONTROL/99-001. 2004. *Co-operative Actions of R&D in EUROCONTROL Action on Airborne Separation Assistance System*. Version 5.1. Available from Internet: <http://www.eurocontrol.int/care-asas/gallery/content/public/docs/asasactionplan.pdf>
- Costello, D. J.; Hagenauer, J.; Imai, H.; Wicker, S. B. 1998. Applications of error-control coding, *IEEE Transactions on Information Theory* 44(6): 2531–2560. <http://dx.doi.org/10.1109/18.720548>
- Elbert, B.; Schiff, M. 2003. *Simulating the Performance of Communication Links with Satellite Transponders*. Available from Internet: http://www.applicationstrategy.com/Communications_simulation.htm
- EUROCONTROL. 2012. *Cascade Programme, ADS-B, WAM*. Available from Internet: <http://www.eurocontrol.int/surveillance/cascade>
- Federal Aviation Administration. 2010. *14 CFR Part 91: Automatic Dependent Surveillance – Broadcast (ADS-B) Out Performance Requirements to Support Air Traffic Control (ATC) Service*. Final Rule. Federal Register, Vol. 75, No. 103.
- ICAO. 2011. *Unmanned Aircraft Systems (UAS)*. Cir 328. AN/190. 38 p. Available from Internet: http://www.icao.int/Meetings/UAS/Documents/Circular%20328_en.pdf
- Iridium Satellites. 2008. Available from Internet: <http://www.highspeedsat.com/iridium-satellite.php>
- Feliz, M. 2012. *Iridium Adds ADS-B to its Iridium NEXT Constellation*. Available from Internet: <http://www.aviationtoday.com/the-checklist/76558.html>
- Kharchenko, V. P.; Barabanov, Y. M.; Grekhov, A. M. 2012a. Modelyuvannya suputnykovogo aviacijnogo zv'yazku, *Visnyk Nacional'nogo Aviacijnogo Universytetu – Proceedings of National Aviation University* (1): 5–13. (in Ukrainian).
- Kharchenko, V. P.; Barabanov, Y. M.; Grekhov, A. M. 2012b. Modelyuvannya suputnykovogo kanalu peredachi ADS-B povidomlen', *Visnyk Nacional'nogo Aviacijnogo Universytetu – Proceedings of National Aviation University* (3): 9–14. (in Ukrainian).
- Kharchenko, V. P.; Barabanov, Y. M.; Grekhov, A. M.; Ivanenko, M. S.; Lobanov, R. I. 2012c. Modelyuvannya v sere-dovyshhi Netcracker Professional 4.1 peredachi ADS-B povidomlen' cherez suputnykovyj kanal komunikaciji Iridium, *Visnyk Nacional'nogo Aviacijnogo Universytetu – Proceedings of National Aviation University* (1): 81–86. (in Ukrainian).
- Kharchenko, V.; Prusov, D. 2012. Analysis of unmanned aircraft systems application in the civil field, *Transport* 27(3): 335–343. <http://dx.doi.org/10.3846/16484142.2012.721395>
- Manual for ICAO Aeronautical Mobile Satellite (Route) Service. Part 2-Iridium. Draft v4.0. 2007. 77 p. Available from Internet: [http://legacy.icao.int/anb/panels/acp/wg/m/iridium_swg/ird-08/ird-swg08-ip05%20-%20ams\(r\)s%20manual%20part%20ii%20v4.0.pdf](http://legacy.icao.int/anb/panels/acp/wg/m/iridium_swg/ird-08/ird-swg08-ip05%20-%20ams(r)s%20manual%20part%20ii%20v4.0.pdf)
- Manual on Detailed Technical Specifications for the Aeronautical Telecommunication Network (ATN). 2010. Doc 9880-AN/466.
- Osborne, W. P.; Xie, Y. 1999. Propagation characterization of LEO/MEO satellite systems at 900–2100 MHz, in *1999 IEEE Emerging Technologies Symposium. Wireless Communications and Systems*. 12–13 April 1999, Richardson, TX, USA, 21.1–21.8. <http://dx.doi.org/10.1109/ETWCS.1999.897339>
- Remotely Piloted Aircraft Systems (RPAS). 2012. Available from Internet: <http://ec.europa.eu/enterprise/sectors/aerospace/uas>
- Roddy, D. 2006. *Satellite Communications*. 4th edition, McGraw-Hill Professional. 636 p.
- RTCA. 2002. *Minimum Aviation System Performance Standards for Automatic Dependent Surveillance Broadcast (ADS-B)*. DO-242A. 203 p.
- RTCA. 1995. *Final Report of RTCA Task Force 3: Free Flight Implementation*.
- Saleh, A. A. M. 1981. Frequency-independent and frequency-dependent nonlinear models of TWT amplifiers, *IEEE Transactions on Communications* 29(11): 1715–1720. <http://dx.doi.org/10.1109/TCOM.1981.1094911>
- Sklar, B. 2001. *Digital Communications: Fundamentals and Applications*. 2nd edition, Prentice Hall. 1079 p.
- Third Unmanned Aircraft Systems (UAS) EU Workshop – Safety. 2011. Organised at EUROCONTROL. Available from Internet: <http://www.eurocontrol.int/events/third-unmanned-aircraft-systems-uas-eu-workshop-safety>
- Towards a European Strategy for the Development of Civil applications of Remotely Piloted Aircraft Systems (RPAS). 2012. SWD(2012) 259 final. 29 p. Available from Internet: <http://register.consilium.europa.eu/pdf/en/12/st13/st13438.en12.pdf>
- Viterbi, A. J. 1971. Convolutional codes and their performance in communication systems, *IEEE Transactions on Communication Technology* 19(5): 751–772. <http://dx.doi.org/10.1109/TCOM.1971.1090700>
- Woolner, P. 2003. *Aircraft-to-Satellite Links Suitable for Transmitting USDA Forest Service Infrared Forest Fire Data: Screening and Feasibility Study*. 28 p. Available from Internet: http://nirops.fs.fed.us/docs/upload/USFS_satcom_report.pdf